Femtosecond excitation correlation spectroscopy of single-walled carbon nanotubes: Analysis based on nonradiative multiexciton recombination processes

Yuhei Miyauchi,[1,2,*] Kazunari Matsuda,[1] and Yoshihiko Kanemitsu[1,3]
[1]*Institute for Chemical Research, Kyoto University, Uji, Kyoto 611-0011, Japan*
[2]*Center for Integrated Science and Engineering, Columbia University, New York, New York 10027, USA*
[3]*Photonics and Electronics Science and Engineering Center, Kyoto University, Kyoto 615-8510, Japan*
(Received 27 August 2009; revised manuscript received 22 October 2009; published 30 December 2009)

We studied the nonlinear time-resolved luminescence signals due to multiexciton recombination processes in single-walled carbon nanotubes (SWNTs) using femtosecond excitation correlation (FEC) spectroscopy. From theoretical analysis of the FEC signals, we found that the FEC signals in the long time range are dominated by the single exciton decay in SWNTs, where the exciton-exciton annihilation process is efficient. Our results provide a simple method to clarify the single exciton decay dynamics in low-dimensional materials.

DOI: 10.1103/PhysRevB.80.235433 PACS number(s): 73.22.−f, 78.67.Ch, 78.47.Cd, 78.47.jc

I. INTRODUCTION

Since the first report in 1981,[1,2] the nonlinear time-resolved photoluminescence (PL) spectroscopy technique termed picosecond or femtosecond excitation correlation (PEC or FEC) has been applied to investigate the carrier and/or exciton dynamics in various semiconductors.[1–17] This method has the benefits of excellent time-resolution, limited only by the pulse width of the laser light used to excite the material, and a simpler experimental setup than the other ultrafast techniques. Theoretical models of the origin of FEC signals are inevitably required for interpretation of the data. Previous studies using the excitation correlation method concerned the recombination lifetimes of carriers[1–7] and excitons,[8] tunneling dynamics,[9–11] bimolecular formation of excitons,[12,13] and transport properties of carriers.[14,15] FEC signals are based on optical nonlinearities in materials. Since single-walled carbon nanotubes (SWNTs) are known to have strong optical nonlinearities, one could apply the FEC method on SWNTs.[16,17]

The exciton-exciton annihilation process dominates the nonlinearity of low-dimensional semiconductor nanostructures with strong Coulomb interactions, such as SWNTs.[18–22] SWNTs have large exciton binding energies (~0.4 eV),[23] and excitons are stable even at room temperature. In addition, very rapid exciton-exciton annihilation processes (of the order 1 ps for only two excitons) have been reported.[21,22] Well-isolated SWNTs show near infrared (IR) PL around 1 eV,[23–27] and the emission energy is inversely proportional to the tube diameter, d. Recent time-resolved measurements by time-correlated single photon counting (TCSPC) method,[28–31] streak camera,[32,33] frequency up conversion,[34] and Kerr gate[18,35] techniques have revealed the PL lifetimes of isolated SWNTs of the order of 10–100 ps. However, the TCSPC measurement is inadequate for the large diameter SWNTs ($d > \sim 0.8$ nm) because of the limit of the sensitive range of Si-based single photon counting avalanche photodiodes, and the sensitivity and time-resolution of near IR streak cameras are low. Although frequency upconversion[34] and Kerr gate[18,35] methods provide excellent time-resolution, these methods involve relatively complicated experimental setups. Hence, the development of alternatives has been eagerly anticipated to measure the ultrafast PL dynamics in SWNTs in the near IR range with good time resolution. Although there has been a report on the FEC measurements of SWNTs in which the interpretation was performed using a stochastic model,[17] no study has reported the analytical expression of the time dependence of the FEC signals that makes the physics behind the FEC signals in SWNTs clearer and makes it easier to interpret the obtained data by this method.

In this paper, we analytically calculate the nonlinear FEC signals arising from the nonradiative exciton-exciton annihilation process, and apply FEC spectroscopy to SWNTs. In Sec. II, we describe a theoretical analysis of the nonlinear FEC signals after presenting a general aspect of the FEC measurement. In Sec. III, we show the experimental procedures and results on SWNTs as a typical material having stable excitons even at room temperature and exhibiting very efficient exciton-exciton annihilation in the strong excitation regime. We analyze the experimental data based on the theoretical scheme presented in Sec. II and successfully derive the single exciton lifetimes in SWNTs. Our results suggest that the FEC signals are dominated by single exciton decay at longer delay times, after the rapid exciton-exciton nonradiative recombination processes. The single exciton lifetimes can be readily determined using the FEC technique in materials where the exciton-exciton annihilation process dominates the optical nonlinearity.

II. THEORETICAL ANALYSIS OF EXCITATION CORRELATION SIGNALS DUE TO RAPID EXCITON-EXCITON ANNIHILATION

The PL correlation signals measured by the FEC method originate from the nonlinearity in the PL intensity as a function of the excitation power. We assume a pair of pump beams with the same power and photon energy, and the beams are modulated at two different frequencies, ω_1 and ω_2, and the nonlinear PL signal from the sample is detected using a lock-in amplifier. When one of the pump beams is blocked, the output signals of the lock-in amplifier are expressed as

$$I_1(t) = I_0 S(t, \omega_1), \tag{1}$$

$$I_2(t) = I_0 S(t, \omega_2), \tag{2}$$

where I_0 is the amplitude of the detected PL intensity, and $S(t, \omega_i)$ are 50% duty cycle square waves with amplitudes between 1 and 0 and frequencies ω_1 and ω_2. Nonlinear response that we detect as the FEC signals occurs only when the two pump beams are on at the same time. The time dependence of this signal can be expressed as

$$I_{\mathrm{PLcor}}(t) = I_{\mathrm{C}}(\tau) S(t, \omega_1) S(t, \omega_2), \tag{3}$$

where $I_{\mathrm{C}}(\tau)$ is the amplitude of the nonlinear correlation signal as a function of the delay time τ between two pump pulses. Then, the total detected signal can be expressed as

$$I_{\mathrm{PLtot}}(t) = I_0[S(t, \omega_1) + S(t, \omega_2)] + I_{\mathrm{C}}(\tau) S(t, \omega_1) S(t, \omega_2). \tag{4}$$

Because the term $S(t, \omega_1)S(t, \omega_2)$ can be decomposed into two components with frequencies $\omega_1 + \omega_2$ and $\omega_1 - \omega_2$, we can separate the contribution of $I_{\mathrm{C}}(\tau)$ by selecting the lock-in response at the sum or difference frequencies. The functional form of $I_{\mathrm{C}}(\tau)$ depends on the mechanism of nonlinearity in the materials.

Here, we consider low dimensional semiconductors where the optical properties are dominated by strongly bound excitons, and the nonlinearity of the PL is caused by exciton-exciton annihilation (Auger nonradiative recombination). This situation is well-known to occur in SWNTs,[18–22,36] which is one of the ideal one-dimensional materials with stable excitons and strong exciton-exciton interactions. The recent study on PL saturation has shown that the effect of absorption saturation is still small even for PL saturation regime.[36] Under strong pump intensity, where the initially generated exciton population in a SWNT by a single pump pulse is more than 1, we assume that the average exciton population N obeys the following rate equations:

$$\frac{dN_{\mathrm{A}}}{dt} = G(t) - \gamma_1 N_{\mathrm{A}} - \gamma_{\mathrm{A}} N_{\mathrm{A}}(N_{\mathrm{A}} - 1), \quad N_{\mathrm{A}} \geq 1, \tag{5}$$

$$\frac{dN_1}{dt} = -\gamma_1 N_1, \quad N_1 \leq 1, \tag{6}$$

where N_{A} and N_1 are exciton populations under $N \geq 1$ and $N \leq 1$ conditions, respectively, γ_{A} is the coefficient determining the nonlinear decay rate $\gamma_{\mathrm{A}} N(N-1)$,[18] γ_1 is the recombination rate for a single exciton, and $G(t)$ is the instantaneous generation function of N_0 (>1) excitons at $t=0$. Equations (5) and (6) give the short-time (nonlinear) and long-time (linear) exciton population functions that correspond to the short and long time limits of the solution of the stochastic model of exciton relaxation in SWNTs,[37] which is valid for the strong excitation conditions studied here. Here, we neglect the fine structure of the exciton levels at room temperature (e.g., bright-dark exciton level splitting),[38–41] and assume that the excitons generated in higher energy states relax into the lowest bright state in a time shorter than the pulse duration, and unity relaxation efficiency. Under these conditions, Eqs. (5) and (6) become

$$N_{\mathrm{A}}(t, N_0) = \frac{1}{\Gamma - \left(\Gamma - \frac{1}{N_0}\right)\exp[-(\gamma_{\mathrm{A}} - \gamma_1)t]}, \quad N_{\mathrm{A}} \geq 1, \tag{7}$$

$$N_1(t, t_1) = \exp[-\gamma_1 (t - t_1)], \quad N_1 \leq 1, \tag{8}$$

where $\Gamma \equiv \gamma_{\mathrm{A}}/(\gamma_{\mathrm{A}} - \gamma_1)$, and t_1 is the time when $N_{\mathrm{A}}(t_1, N_0) = 1$. t_1 is expressed as

$$t_1 = \frac{1}{\gamma_{\mathrm{A}} - \gamma_1} \ln\left[\frac{N_0 \Gamma - 1}{N_0(\Gamma - 1)}\right]. \tag{9}$$

Equations (7) and (8) are smoothly connected at $t = t_1$, and this modeling of the time dependent exciton population enables us to obtain analytical expression of the FEC decay curves.

For a single-pulse excitation, the exciton number $N_{\mathrm{S}}(t, N_0)$ is expressed as

$$N_{\mathrm{S}}(t, N_0) = [1 - \Theta(t - t_1)] N_{\mathrm{A}}(t, N_0) + \Theta(t - t_1) N_1(t - t_1), \tag{10}$$

where $\Theta(t)$ is the Heaviside step function for which $\Theta(0) = 1$ is defined. For a two-pulse excitation with a delay time τ, the exciton number, $N_{\mathrm{T}}(t, N_0, \tau)$, is given by

$$N_{\mathrm{T}}(t, N_0, \tau) = \Theta(t)[1 - \Theta(t - \tau)] N_{\mathrm{S}}(t, N_0) + \Theta(t - \tau) N_{\mathrm{S}}[t - \tau, N_0 + N_{\mathrm{S}}(\tau, N_0)]. \tag{11}$$

For recombination of the $N_{\mathrm{T}}(t, N_0, \tau)$ excitons, the total PL intensity $I_{\mathrm{PL}}(N_0, \tau)$ is described as

$$I_{\mathrm{PL}}(N_0, \tau) = \int_0^\infty \gamma_{\mathrm{R}} N_{\mathrm{T}}(t, N_0, \tau) dt, \tag{12}$$

where γ_{R} is the radiative decay rate.

The correlation (FEC) signal $I_{\mathrm{C}}(N_0, \tau)$ is defined as

$$I_{\mathrm{C}}(N_0, \tau) = I_{\mathrm{PL}}(N_0, \tau) - I_{\mathrm{PL}}(N_0, \infty). \tag{13}$$

To evaluate $I_{\mathrm{C}}(N_0, \tau)$, we calculate $I_{\mathrm{PL}}(N_0, \tau)$ according to Eq. (12). Using $N_{\mathrm{S}}(t, N_0)$, Eq. (12) becomes

$$I_{\mathrm{PL}}(N_0, \tau) = \int_0^\tau \gamma_{\mathrm{R}} N_{\mathrm{S}}(t, N_0) dt + \int_\tau^\infty \gamma_{\mathrm{R}} N_{\mathrm{S}}[t - \tau, N_0 + N_{\mathrm{S}}(\tau, N_0)] dt. \tag{14}$$

$I_{\mathrm{PL}}(N_0, \tau)$ is calculated for $\tau < t_1$ and $\tau \geq t_1$ as

$$I_{\mathrm{PL}}(N_0, \tau) = \frac{\gamma_{\mathrm{R}}}{\gamma_{\mathrm{A}}} \ln\left(\frac{\{N_0 \Gamma \exp[(\gamma_{\mathrm{A}} - \gamma_1)\tau] - N_0 \Gamma + 1\}\{[N_0 + N_{\mathrm{A}}(\tau, N_0)]\Gamma - 1\}}{\Gamma - 1}\right) + \frac{\gamma_{\mathrm{R}}}{\gamma_1}, \quad \tau < t_1, \tag{15}$$

$$I_{\mathrm{PL}}(N_0,\tau)=\frac{\gamma_{\mathrm{R}}}{\gamma_{\mathrm{A}}}\ln\left(\frac{[N_0\Gamma-1]\{[N_0+N_1(\tau,N_0)]\Gamma-1\}}{(\Gamma-1)^2}\right)+\frac{\gamma_{\mathrm{R}}}{\gamma_1}\{2-\exp[-\gamma_1(\tau-t_1)]\},\quad \tau\geq t_1. \tag{16}$$

$I_{\mathrm{PL}}(N_0,\infty)$ is obtained by taking the limit of $\tau\rightarrow\infty$ as

$$I_{\mathrm{PL}}(N_0,\infty)=2\left[\frac{\gamma_{\mathrm{R}}}{\gamma_{\mathrm{A}}}\ln\left(\frac{N_0\Gamma-1}{\Gamma-1}\right)+\frac{\gamma_{\mathrm{R}}}{\gamma_1}\right]. \tag{17}$$

The $I_{\mathrm{C}}(N_0,\tau)$ is thus calculated according to Eq. (13) as

$$I_{\mathrm{C}}(N_0,\tau)=-\frac{\gamma_{\mathrm{R}}}{\gamma_1}+\frac{\gamma_{\mathrm{R}}}{\gamma_{\mathrm{A}}}\ln\left(\frac{\{N_0\Gamma\exp[(\gamma_{\mathrm{A}}-\gamma_1)\tau]-N_0\Gamma+1\}\{[N_0+N_{\mathrm{A}}(\tau,N_0)]\Gamma-1\}(\Gamma-1)}{(N_0\Gamma-1)^2}\right),\quad \tau<t_1, \tag{18}$$

$$I_{\mathrm{C}}(N_0,\tau)=-\frac{\gamma_{\mathrm{R}}}{\gamma_1}\exp[-\gamma_1(\tau-t_1)]+\frac{\gamma_{\mathrm{R}}}{\gamma_{\mathrm{A}}}\ln\left\{\frac{[N_0+N_1(\tau,t_1)]\Gamma-1}{N_0\Gamma-1}\right\},\quad \tau\geq t_1. \tag{19}$$

Note that the second logarithm term in Eq. (19) is considerably smaller than the first exponential term for $N_0\gg 1$ and $\gamma_{\mathrm{A}}\gg\gamma_1$. The simplified form of $I_{\mathrm{C}}(N_0,\tau)$ in this condition is, therefore,

$$I_{\mathrm{C}}(N_0,\tau)=-\frac{\gamma_{\mathrm{R}}}{\gamma_1}\left(\frac{N_0\Gamma-1}{N_0(\Gamma-1)}\right)^{\gamma_1/(\gamma_{\mathrm{A}}-\gamma_1)}\exp(-\gamma_1\tau). \tag{20}$$

Hence, the correlation signals for $\tau\geq t_1$, $N_0\gg 1$ and $\gamma_{\mathrm{A}}\gg\gamma_1$ can be approximated as simple monoexponential decay with the total exciton recombination rate γ_1.

The theoretical result can be qualitatively understood as follows. Figures 1(a) and 1(b) show schematic diagrams of the mechanism of FEC signals due to exciton–exciton annihilation for $\tau\gg\gamma_1^{-1}$ and $\tau\sim\gamma_1^{-1}$ under the conditions $N_0\gg 1$ and $\gamma_{\mathrm{A}}\gg\gamma_1$, respectively. The first pulse generates N_0 excitons at $t=0$, and the multiexcitons quickly annihilate due to rapid exciton-exciton nonradiative recombination processes, followed by the decay of the single surviving exciton. At longer delay time $\tau\gg\gamma_1^{-1}$ in Fig. 1(a), no correlation exists between the PL signals generated by the first and second pulse; the nonlinear correlation signal is zero. After the shorter delay time, $\tau\sim\gamma_1^{-1}$, in Fig. 1(b), the second pulse additionally generates N_0 excitons, and the total generated, $N_0+N_1(\tau)$, $[N_1(\tau)<1]$ again quickly annihilate. If we neglect the integrated PL intensity in the very short time period of the fast nonlinear decay $(0\leq\tau\leq t_1)$, the second pulse instantaneously removes the $N_1(\tau)$ excitons generated by the first pulse. The difference of $I_{\mathrm{PL}}(N_0,\tau)$ and $I_{\mathrm{PL}}(N_0,\infty)$ thus corresponds to the integration of the removed excitons from $t=\tau$ to ∞ as

$$I_{\mathrm{C}}(N_0,\tau)\approx-\int_{\tau}^{\infty}\gamma_{\mathrm{R}}N_1(t)dt. \tag{21}$$

Hence, if $N_1(t)$ is the monoexponential function, the correlation signal can be approximated by a monoexponential function in this case.

Figures 2(a) and 2(b) show simulated correlation signals using Eqs. (18) and (19) for various N_0 values with the parameters of $\gamma_{\mathrm{A}}/\gamma_1=10$ and $\gamma_{\mathrm{A}}/\gamma_1=100$, respectively. These values were selected for simulation because the reported nonlinear annihilation coefficients γ_{A} are of the order of 1 ps^{-1} (Refs. 21 and 22) for SWNTs, which is about one to two orders of magnitude larger than the single exciton recombination rates.[28–35] The upward direction on the vertical axis in the figures indicates that the FEC signals have a negative sign. A monoexponential decay is also shown in Figs. 2(a) and 2(b) for comparison. The weak dependence on N_0 appears only in the very short delay time range [Figs. 2(a) and 2(b)], when the single exciton recombination rate is much smaller than the exciton–exciton annihilation rate. After a delay time longer than $\sim\gamma_{\mathrm{A}}^{-1}$, the decay curve is almost perfectly coincident with the monoexponential decay with the single-exciton decay rate γ_1. This indicates that the single exciton decay can be readily studied from the FEC signals as long as the condition $\gamma_{\mathrm{A}}\gg\gamma_1$ is satisfied. Moreover, we can check whether these conditions are satisfied by measuring the excitation power dependence of the FEC decay curves.

III. EXPERIMENTAL RESULTS OF FEMTOSECOND EXCITATION CORRELATION SIGNALS FROM SINGLE-WALLED CARBON NANOTUBES

The SWNTs synthesized by the alcohol catalytic chemical vapor deposition (ACCVD) method at 850 °C (Ref. 42) were isolated by dispersion in a toluene solution with 0.07 wt% poly[9,9-dioctylfluorenyl-2,7-diyl] (PFO) (PFO-dispersed SWNTs), 60 min of moderate bath sonication, 15 min of vigorous sonication with a tip-type sonicator, and centrifugation at an acceleration of 13 000 g for 5 min, according to the procedure developed by Nish *et al.*[43] To check the sample quality, we measured a PL excitation map and an optical absorption spectrum of PFO-dispersed SWNTs, respectively (not shown here).[44] We observed the very low underlying background in the absorption spectrum and pronounced absorption peaks, which are a signature of excellently isolated, high quality dispersion of SWNTs with an absence of bundled SWNTs, residual impurities, or other amorphous or graphitic carbon compounds.[43] The optical measurements indicate that only several types of chiral indi-

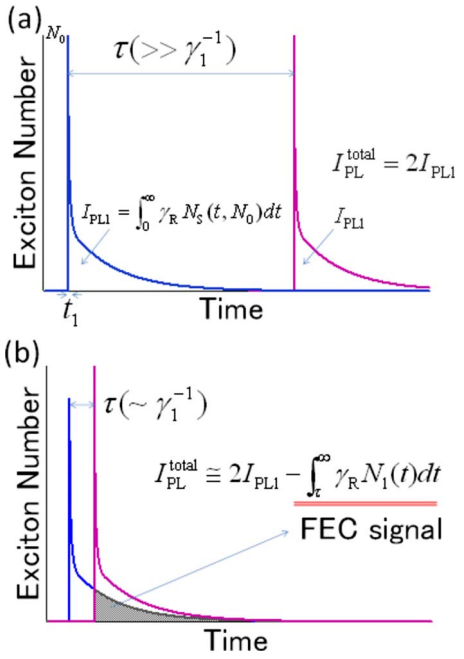

FIG. 1. (Color online) Schematic diagram of the mechanism of FEC signals due to exciton-exciton annihilation for (a) $\tau \gg \gamma_1^{-1}$ and (b) $\tau \sim \gamma_1^{-1}$ under the conditions of $N_0 \gg 1$ and $\gamma_A \gg \gamma_1$. The shaded area in (b) corresponds to the FEC signal at decay time τ.

ces (n, m) (Ref. 45) are included in the sample. For comparison, we also prepared SWNTs by dispersion in D_2O using 0.5 wt% sodium dodecyl benzene sulfonate (SDBS) (SDBS-dispersed SWNTs) with 30 min of vigorous sonication and ultracentrifugation at an acceleration of 150 000 g for 2 h, according to the procedure in Ref. 24.

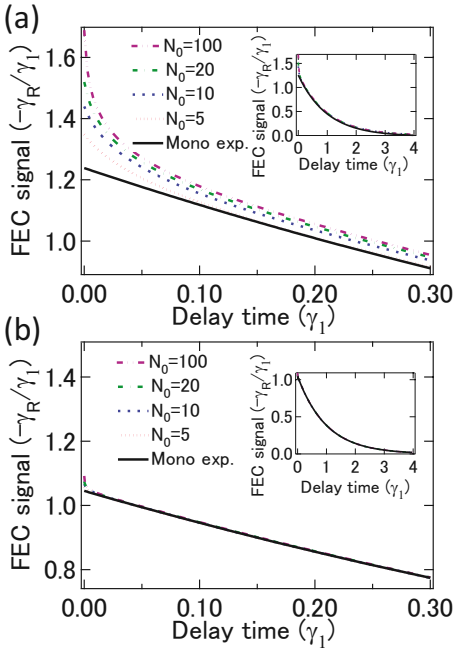

FIG. 2. (Color online) Simulated FEC signals for various N_0 for (a) $\gamma_A/\gamma_1 = 10$ and (b) $\gamma_A/\gamma_1 = 100$. Monoexponential FEC decays are plotted for comparison. Insets show the FEC signals in the long delay time range.

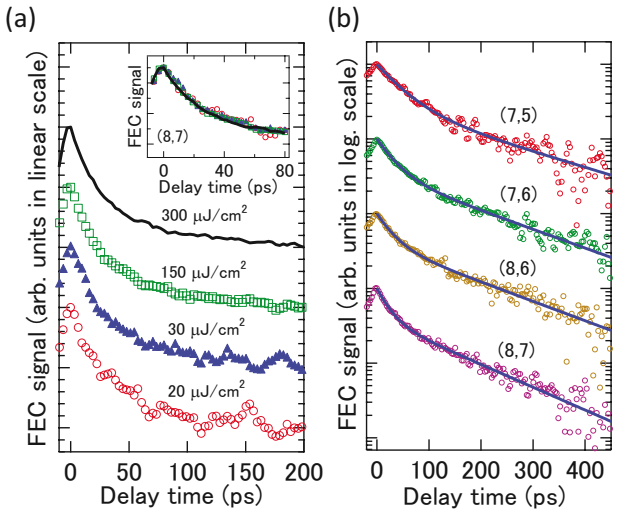

FIG. 3. (Color online) (a) FEC signals for the (8, 7) SWNTs of the PFO-dispersed sample measured under 1.66 eV excitation conditions from ~20 to 300 $\mu J/cm^2$. The vertical axis is in linear scale. Inset compares the first components of each FEC signal. (b) FEC signals for (7, 5), (7, 6), (8, 6), and (8, 7) SWNTs, respectively. The fitted curves using the double-exponential function in Eq. (23) are shown as solid lines. The vertical axis is in logarithmic scale.

We measured the delay time dependence of FEC signals for SWNTs. The SWNTs were excited with ultrashort pulses from a Ti:sapphire laser of central wavelength 745 nm, repetition rate 80 MHz, pulse duration ~150 fs, and spectral width 8 nm. The two beams were separated by a delay time τ and chopped at 800 and 670 Hz, respectively, then collinearly focused to a spot size of ~10 μm. Only the PL signal components modulated at the sum frequency (1470 Hz) were detected using a photomultiplier and a lock-in amplifier, following dispersion of the PL using a monochromator. The measurements were carried out under the excitation of ~20 to 300 $\mu J/cm^2$. The background subtraction of the FEC signals was based on the signal values at delay times more than ~0.7–1 ns, which is considerably longer than the PL lifetimes of SWNTs. We have confirmed the validity of the background subtraction from the experimental observation that no PL signal in the range of more than ~600 ps exists using a near IR streak camera with the time resolution of ~100 ps.

Figure 3(a) shows the excitation power dependence of the FEC signals for PFO-dispersed (8, 7) SWNTs as a function of the delay time. Inset of Fig. 3(a) compares the each FEC decay curve normalized at $\tau = 0$. We observed no substantial change in the FEC decay curve with the excitation power density in the range ~20 to 300 $\mu J/cm^2$, which is consistent with previous results for the micelle-encapsulated SWNTs in D_2O.[16] Assuming the recently reported absorption cross section of E_{22} excitons ~110 $nm^2/\mu m$,[30] the number of excitons generated by a single pulse in our experiment was roughly estimated as $\sim 10^1 - 10^2$ excitons for the excitation density of ~20 to 300 $\mu J/cm^2$. From this estimate, we can confirm that the theoretical analysis in Sec. II is applicable to the experimentally obtained FEC signals. Moreover, this lack of excitation power dependence is a strong indication of the

very rapid exciton-exciton annihilation processes in SWNTs described in Sec. II.

Figure 3(b) shows the FEC signals for PFO-dispersed SWNTs with various chiral indices. We found that the decay curves are well described by a double-exponential function (solid line) after subtracting the background signals for all the observed (n, m) SWNTs. The double-exponential PL decay even in a single SWNT with relatively long PL lifetimes was recently observed.[30,46] Since we observed no excitation power dependence of the FEC decay curve [as shown in Fig. 3(a)], we can use Eq. (21) for the analysis of the FEC signals. The exciton population obeying the double-exponential decay as

$$N_1(t) = C\exp(-t/\tau_A) + (1-C)\exp(-t/\tau_B),$$

$$0 \le C \le 1, \quad \tau_A < \tau_B \tag{22}$$

gives the FEC signal $I_C(\tau)$ calculated using Eq. (21) as

$$I_C(\tau) \propto -[C\tau_A \exp(-\tau/\tau_A) + (1-C)\tau_B \exp(-\tau/\tau_B)], \tag{23}$$

where C is the fractional amplitude of the fast decay component. For (7, 5) SWNTs, we fitted the experimental results of FEC signals and obtained $C \cong 0.92$, $\tau_A \cong 45$ ps and $\tau_B \cong 200$ ps. Here, we define the effective PL lifetime as $\tau_{EFF} = C\tau_A + (1-C)\tau_B$. The τ_{EFF} obtained for (7, 5) was 58 ± 21 ps. We have also checked that τ_{EFF} is consistent with that obtained by the streak camera ($\sim$60 ps). Furthermore, these results are quite similar to the recently reported values for high quality single (6, 5) SWNTs in surfactant suspension measured by TCSPC.[30] This suggests that the single exciton decay can be properly measured by the FEC technique for high quality SWNTs used here. We also measured the PL lifetimes of various (n, m) species, as shown in Fig. 3(b). The τ_{EFF} values obtained for (7, 6), (8, 6), and (8, 7) SWNTs were 43 ± 9, 42 ± 12, and 33 ± 9 ps, respectively. Because the radiative lifetimes of excitons in SWNTs are of the order of 1–10 ns,[44] the PL lifetimes on the order of several tens of picoseconds are attributed to nonradiative decay due to extrinsic effects such as defects, doping, and impurities.

In order to further study the nonradiative processes, we also performed the effective PL lifetime measurements of SWNTs dispersed in D_2O using SDBS. Figure 4 compares the diameter dependence of the effective PL lifetimes of PFO-dispersed and SDBS-dispersed SWNTs. The PFO-dispersed SWNTs have longer PL lifetimes than the SDBS-dispersed SWNTs in smaller diameter range ($d < 1$ nm). When the ensemble averages could be dominated by a minority of SWNTs with bright PL, the total average PL lifetimes of SDBS-dispersed SWNTs might be smaller than the values obtained here considering the large background signals in optical absorption spectra.[44] The PFO-dispersed SWNTs tend to have shorter PL lifetimes with increasing the diameters. On the other hand, the PL lifetimes of SDBS-dispersed SWNTs are almost constant in this diameter range.

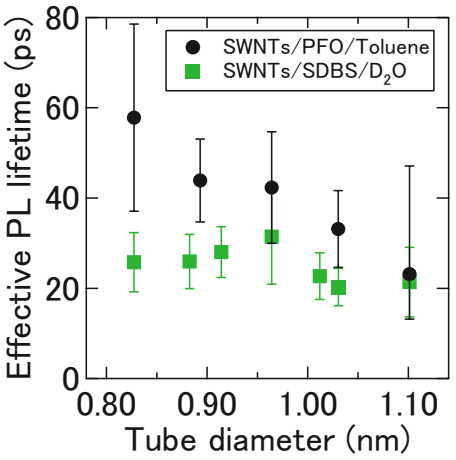

FIG. 4. (Color online) Effective PL lifetimes of SWNTs prepared with different dispersion methods measured using FEC method. The effective PL lifetimes are determined using the double-exponential function in Eq. (23).

These results suggest that the effective PL lifetimes are determined by the nonradiative process and the dispersion method of SWNTs strongly affects the exciton nonradiative decay rates. Because the larger diameter SWNTs ($d > 1$ nm) are important for applications such as optical communication devices, suppression of the nonradiative decay and improvement of the PL quantum yields for larger diameter SWNTs is highly desirable. In addition to the usefulness of the FEC technique for fundamental physics researches, PL lifetime measurement using FEC will enable easy sample-quality screening of large diameter SWNTs with PL emission energies less than $\sim$1 eV.

IV. SUMMARY

We have demonstrated the theoretical analysis of FEC signals originating from nonradiative exciton-exciton annihilation processes. We found that the FEC signals are dominated by the single exciton decay dynamics when the nonlinear exciton-exciton annihilation process is much faster than the single exciton decay. We measured the FEC signals in SWNTs and determined the single-exciton decay lifetimes. Our results suggest that FEC spectroscopy, with advantages in terms of the time resolution and simple experimental setup, is very useful for the exciton lifetime measurement in low-dimensional materials with rapid exciton-exciton annihilation.

ACKNOWLEDGMENTS

The authors would like to thank S. Noda and K. Ishizaki (Kyoto University) for their experimental support in using the IR streak camera. One of the authors (Y.M.) was financially supported by JSPS (Grant No. 20-3712). Part of this work was supported by JSPS KAKENHI (Grant No. 20340075) and MEXT KAKENHI (Grants No. 20048004 and No. 20104006) of Japan.

*Corresponding author; y.miyauchi@at7.ecs.kyoto-u.ac.jp

[1] D. Rosen, A. G. Doukas, Y. Budansky, A. Katz, and R. R. Alfano, Appl. Phys. Lett. **39**, 935 (1981).
[2] D. von der Linde, J. Kuhl, and E. Rosengart, J. Lumin. **24-25**, 675 (1981).
[3] M. B. Johnson, T. C. McGill, and A. T. Hunter, J. Appl. Phys. **63**, 2077 (1988).
[4] H. J. W. Eakin and J. F. Ryan, J. Lumin. **40-41**, 553 (1988).
[5] A. M. de Paula, R. A. Taylor, C. W. W. Bradley, A. J. Turberfield, and J. F. Ryan, Superlattices Microstruct. **6**, 199 (1989).
[6] J. L. A. Chilla, O. Buccafusca, and J. J. Rocca, Phys. Rev. B **48**, 14347 (1993).
[7] R. Kumar and A. S. Vengurlekar, Phys. Rev. B **54**, 10292 (1996).
[8] M. Jørgensen and J. M. Hvam, Appl. Phys. Lett. **43**, 460 (1983).
[9] M. K. Jackson, M. B. Johnson, D. H. Chow, T. C. McGill, and C. W. Nieh, Appl. Phys. Lett. **54**, 552 (1989).
[10] N. Sawaki, R. A. Höpfel, E. Gornik, and H. Kano, Appl. Phys. Lett. **55**, 1996 (1989).
[11] V. Emiliani, S. Ceccherini, F. Bogani, M. Colocci, A. Frova, and S. S. Shi, Phys. Rev. B **56**, 4807 (1997).
[12] R. Strobel, R. Eccleston, J. Kuhl, and K. Köhler, Phys. Rev. B **43**, 12564 (1991).
[13] S. Pau, J. Kuhl, M. A. Khan, and C. J. Sun, Phys. Rev. B **58**, 12916 (1998).
[14] R. Christanell and R. A. Höpfel, Superlattices Microstruct. **5**, 193 (1989).
[15] E. Okuno, T. Hori, N. Sawaki, I. Akasaki, and R. A. Höpfel, Jpn. J. Appl. Phys., Part 2 **31**, L148 (1992).
[16] H. Hirori, K. Matsuda, Y. Miyauchi, S. Maruyama, and Y. Kanemitsu, Phys. Rev. Lett. **97**, 257401 (2006).
[17] Y.-F. Xiao, T. Q. Nhan, M. W. B. Wilson, and J. M. Fraser, Proc. SPIE **7201**, 720111 (2009).
[18] F. Wang, G. Dukovic, E. Knoesel, L. E. Brus, and T. F. Heinz, Phys. Rev. B **70**, 241403(R) (2004).
[19] Y.-Z. Ma, L. Valkunas, S. L. Dexheimer, S. M. Bachilo, and G. R. Fleming, Phys. Rev. Lett. **94**, 157402 (2005).
[20] L. Valkunas, Y.-Z. Ma, and G. R. Fleming, Phys. Rev. B **73**, 115432 (2006).
[21] F. Wang, Y. Wu, M. S. Hybertsen, and T. F. Heinz, Phys. Rev. B **73**, 245424 (2006).
[22] K. Matsuda, T. Inoue, Y. Murakami, S. Maruyama, and Y. Kanemitsu, Phys. Rev. B **77**, 033406 (2008).
[23] F. Wang, G. Dukovic, L. E. Brus, and T. F. Heinz, Science **308**, 838 (2005).
[24] M. J. O'Connell, S. M. Bachilo, C. B. Huffman, V. C. Moore, M. S. Strano, E. H. Haroz, K. L. Rialon, P. J. Boul, W. H. Noon, C. Kittrell, J. Ma, R. H. Hauge, R. B. Weisman, and R. E. Smalley, Science **297**, 593 (2002).
[25] S. M. Bachilo, M. S. Strano, C. Kittrell, R. H. Hauge, R. E. Smalley, and R. B. Weisman, Science **298**, 2361 (2002).
[26] J. Lefebvre, Y. Homma, and P. Finnie, Phys. Rev. Lett. **90**, 217401 (2003).
[27] J. Lefebvre, J. M. Fraser, P. Finnie, and Y. Homma, Phys. Rev. B **69**, 075403 (2004).
[28] A. Hagen, M. Steiner, M. B. Raschke, C. Lienau, T. Hertel, H. Qian, A. J. Meixner, and A. Hartschuh, Phys. Rev. Lett. **95**, 197401 (2005).
[29] M. Jones, W. K. Metzger, T. J. McDonald, C. Engtrakul, R. J. Ellingson, G. Rumbles, and M. J. Heben, Nano Lett. **7**, 300 (2007).
[30] S. Berciaud, L. Cognet, and B. Lounis, Phys. Rev. Lett. **101**, 077402 (2008).
[31] T. Gokus, A. Hartschuh, H. Harutyunyan, M. Allegrini, F. Hennrich, M. Kappes, A. A. Green, M. C. Hersam, P. T. Araújo, and A. Jorio, Appl. Phys. Lett. **92**, 153116 (2008).
[32] A. Hagen, G. Moos, V. Talalaev, and T. Hertel, Appl. Phys. A: Mater. Sci. Process. **78**, 1137 (2004).
[33] S. Berger, C. Voisin, G. Cassabois, C. Delalande, P. Roussignol, and X. Marie, Nano Lett. **7**, 398 (2007).
[34] Y.-Z. Ma, J. Stenger, J. Zimmermann, S. M. Bachilo, R. E. Smalley, R. B. Weisman, and G. R. Fleming, J. Chem. Phys. **120**, 3368 (2004).
[35] F. Wang, G. Dukovic, L. E. Brus, and T. F. Heinz, Phys. Rev. Lett. **92**, 177401 (2004).
[36] Y. Murakami and J. Kono, Phys. Rev. Lett. **102**, 037401 (2009).
[37] A. V. Barzykin and M. Tachiya, J. Phys.: Condens. Matter **19**, 065105 (2007).
[38] H. Zhao and S. Mazumdar, Phys. Rev. Lett. **93**, 157402 (2004).
[39] R. Matsunaga, K. Matsuda, and Y. Kanemitsu, Phys. Rev. Lett. **101**, 147404 (2008).
[40] A. Srivastava, H. Htoon, V. I. Klimov, and J. Kono, Phys. Rev. Lett. **101**, 087402 (2008).
[41] O. N. Torrens, M. Zheng, and J. M. Kikkawa, Phys. Rev. Lett. **101**, 157401 (2008).
[42] S. Maruyama, R. Kojima, Y. Miyauchi, S. Chiashi, and M. Kohno, Chem. Phys. Lett. **360**, 229 (2002).
[43] A. Nish, J.-Y. Hwang, J. Doig, and R. J. Nicholas, Nat. Nanotechnol. **2**, 640 (2007).
[44] Y. Miyauchi, H. Hirori, K. Matsuda, and Y. Kanemitsu, Phys. Rev. B **80**, 081410(R) (2009).
[45] R. Saito, G. Dresselhaus, and M. S. Dresselhaus, *Physical Properties of Carbon Nanotubes* (Imperial College Press, London, 1998).
[46] The single SWNT in Refs. 28 and 31 showed the monoexponential PL decay and a distribution of decay times even for SWNTs with the same chirality. In this case, the multiexponential decay could be expected for SWNTs ensembles. This suggests that the different SWNTs with different qualities could have different PL decay dynamics.